Chemical Science

ROYAL SOCIETY OF CHEMISTRY

EDGE ARTICLE

View Article Online
View Journal | View Issue

Cite this: *Chem. Sci.*, 2024, **15**, 14406

All publication charges for this article have been paid for by the Royal Society of Chemistry

Received 29th May 2024
Accepted 27th July 2024

DOI: 10.1039/d4sc03518f

rsc.li/chemical-science

Reactivity of the phosphaethynolate anion with stabilized carbocations: mechanistic studies and synthetic applications†‡

Thi Hong Van Nguyen,[a] Saloua Chelli,[a] Sonia Mallet-Ladeira,[b] Martin Breugst *[c] and Sami Lakhdar *[a]

The reactivity of sodium phosphaethynolate Na(OCP) towards various Mayr's reference electrophiles was investigated using conventional UV-visible and laser-flash photolysis techniques. The kinetic data, along with density functional theory (DFT) calculations, enabled the first experimental quantification of the phosphorus nucleophilicity of $[OCP]^-$. Product studies of these reactions demonstrate the formation of secondary as well as tertiary phosphines. The mechanism of this unprecedented phosphorus-atom transfer reaction is thoroughly discussed, with key intermediates successfully isolated and characterized. Importantly, some bulky secondary phosphine oxides synthesized using this approach, have demonstrated high efficiency as ligands in the Suzuki coupling reaction.

Introduction

The exploration of practical, simple, robust, and sustainable approaches for forming carbon-phosphorus bonds constitutes a vibrant research domain for both academia and industry.[1] This significance arises from the importance of organophosphorus compounds in many areas, spanning from catalysis to medicinal chemistry and materials sciences.[2] Typically, PCl_3 serves as a common starting material from which the majority of organophosphorus molecules can be synthesized. However, the generation of HCl as a side product has spurred efforts to identify alternative phosphorus precursors that are easily accessible and manufactured on a large scale.[3] In this context, phosphinates and related derivatives,[4] as well as white phosphorus (P_4)[5] have garnered attention in recent decades as PCl_3 surrogates, given their potential to be converted into valuable organophosphorus molecules. Phosphaethynolate anion, denoted as $[OCP]^-$, the phosphorus analog of well-studied cyanate anion, has emerged recently as a potential phosphorus precursor.[6] Scheme 1a summarizes selected examples of the use of $[OCP]^-$ for the synthesis of interesting organophosphorus molecules. From the reactivity perspective, $[OCP]^-$ possesses two nucleophilic centers (oxygen and phosphorus) that facilitate the formation of phosphaalkynes[7] or phosphaketenes,[8] serving as key intermediates for the synthesis of organic and organometallic phosphorus compounds (Scheme 1b).

Although the synthesis of $[OCP]^-$ was initially reported nearly thirty years ago by Becker *et al.*,[9] its utilization in

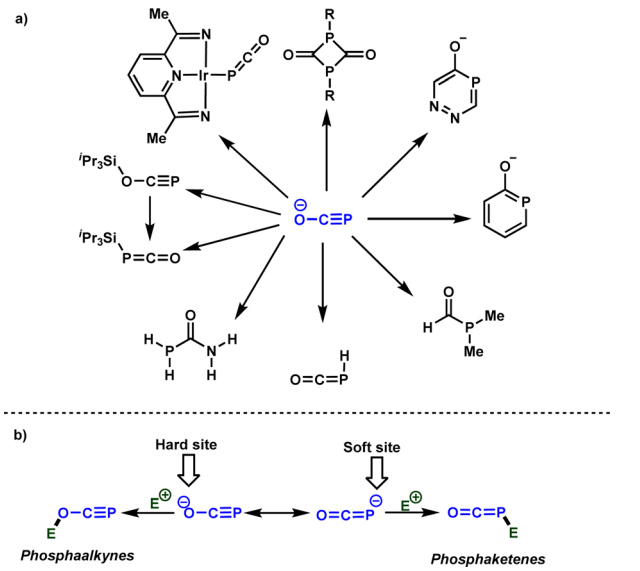

Scheme 1 (a) Selected examples of the use of $[OCP]^-$ for the synthesis of organophosphorus molecules, (b) ambident reactivity of $[OCP]^-$ with electrophiles.

[a]*CNRS, Université Paul Sabatier, Laboratoire Hetérochimie Fondamentale et Appliquée (LHFA, UMR5069), 118 Route de Narbonne, 31062 Cedex 09 Toulouse, France. E-mail: sami.lakhdar@univ-tlse3.fr*

[b]*Institut de Chimie de Toulouse (FR 2599), 118 Route de Narbonne, 31062 Cedex 09 Toulouse, France*

[c]*Institut für Chemie, Technische Universität Chemnitz, 09111 Chemnitz, Germany. E-mail: martin.breugst@chemie.tu-chemnitz.de*

† The article is dedicated to Dr Gilles Dujardin (CNRS, University of Le Mans) on the occasion of his retirement.

‡ Electronic supplementary information (ESI) available. CCDC 2332101–2332103. For ESI and crystallographic data in CIF or other electronic format see DOI: https://doi.org/10.1039/d4sc03518f

inorganic and organic chemistry faced limited development during that period, likely attributed to challenges in reproducing its synthesis on a large scale and the sensitivity of the anion to moisture and air. A noteworthy resurgence in the chemistry of the phosphaethynolate anion has occurred in the last decade, driven by seminal contributions of Grützmacher and Goicoechea groups.[10] These reports independently presented efficient procedures for synthesizing stable phosphaethynolate anion, overcoming previous limitations. Consequently, $[OCP]^-$ has emerged as an appealing phosphorus transfer agent, demonstrating efficiency in the synthesis of numerous organophosphorus molecules and phosphorus-based transition metal complexes.[11]

It is obvious that the rational design of new reactions involving $[OCP]^-$ as a nucleophile necessitates a comprehensive understanding of its ambident reactivity. In 2014, Grützmacher and Benkő elucidated this ambident reactivity by reacting $[OCP]^-$ with iPr_3Si–OTf, yielding the phosphaalkyne and phosphaketene, which were fully characterized (Scheme 1a).[12] It was concluded that while the oxygen attack is kinetically controlled, the phosphorus attack is thermodynamically controlled. Very recently, the Benkő's group employed Marcus theory to rationalize the ambident reactivity of $[OCP]^-$ towards carbon electrophiles. Their results indicated a lower intrinsic barrier for the oxygen attack, highlighting the kinetic preference of oxygen attacks.[13]

Building upon these insights and drawing inspiration from precedent contributions by Mayr and coworkers,[14] which revealed that the ambident reactivity of various nucleophiles does not follow the well-established Hard and Soft Acids and Bases theory (HSAB),[15] we embarked on investigating the reactivity of $[OCP]^-$ towards Mayr's reference electrophiles. The objective is to gain deeper insights into the factors controlling the reactivity of this anion, which is crucial for unlocking its synthetic potential (Table 1).

In previous investigations, Mayr *et al.* have shown that numerous nucleophile–electrophile combinations can simply be described by the three parameters eqn (1), where k_2 measures the second-order rate constant of the reaction of an electrophile with a nucleophile, N and s_N are nucleophilicity parameters, and E is the electrophilicity parameter.[18]

$$\log k_2\ (20\ ^\circ\mathrm{C}) = s_N(E + N) \quad (1)$$

Our investigation commences with the synthesis of sodium phosphaethynolate using a protocol outlined in Scheme 2. This method, previously described by Grützmacher,[12] utilizes inexpensive precursors (sodium, red phosphorus, *t*BuOH, ethylene carbonate).[12] The target compound, $Na(dioxane)_{2.5}(OCP)$ was successfully obtained on a gram scale. As ion pairing should not be important under the low concentrations used in the kinetic studies, $[Na(OCP)](dioxane)_{2.5}$ will be referred to as Na(OCP) throughout this article.

The reaction of Na(OCP) with different reference electrophiles were carried out in acetonitrile at 20 °C, under pseudo-first-order conditions, by using at least 10 equivalents of the nucleophile with respect to the electrophile. Rates of those reactions were determined either by studying the kinetics of laser-flash photolytically generated benzhydrylium ions or conventional UV-visible spectrophotometry using stable quinone methides or benzhydrylium ions.

Following previous investigations by Mayr *et al.*,[19] the carbocation **1j** was generated photolytically upon irradiation of the

Table 1 Reference electrophiles employed for the determination of the nucleophilicity parameters of Na(OCP), their electrophilicity

Electrophile		Electrophilicity, E
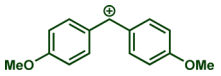	**1a**	0[a]
	**1b**	−3.72[b]
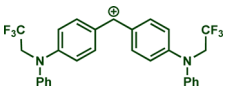	**1c**	−3.85[a]
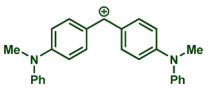	**1d**	−5.89[a]
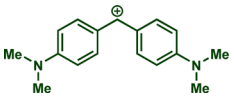	**1e**	−7.02[a]
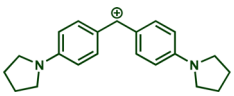	**1f**	−7.69[a]
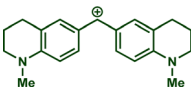	**1g**	−8.22[a]
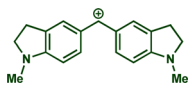	**1h**	−8.76[a]
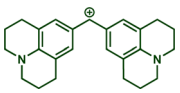	**1i**	−9.45[a]
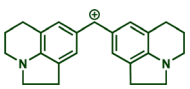	**1j**	−10.04[a]
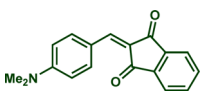	**1k**	−13.56[a]
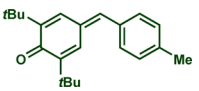	**1l**	−15.83[a]
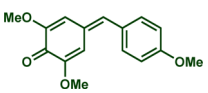	**1m**	−16.38[a]
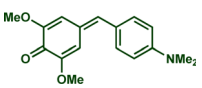	**1n**	−17.18[a]

[a] Taken from ref. 16. [b] Taken from ref. 17.

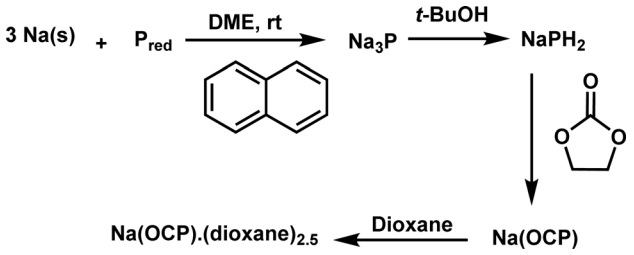

Scheme 2 Synthesis of sodium phosphaethynolate.

corresponding phosphonium salt with a 7 ns laser pulse at 266 nm (see ESI‡). In the presence of a large excess of Na(OCP), one can follow the monoexponentional decays of the absorbance of **1j** ($\lambda_{max} = 635$ nm), from which the rate constants k_{obs} (s^{-1}) are obtained (Fig. 1a). Interestingly, plots of k_{obs} *versus* the Na(OCP) concentrations gave linear correlations (Fig. 1b), and the resulting slopes yielded the second-order rate constants k_2 (L mol^{-1} s^{-1}) which are listed in Table 2. To investigate the role of the counterion on the reactivity of Na(OCP) with benzhydrylium ions, reactions of the former with the carbocation **1n** were studied in the presence of the crown ether 15-crown-5. However, under these conditions, only a very small change in the second-order rate constant was noticed, indicating that the

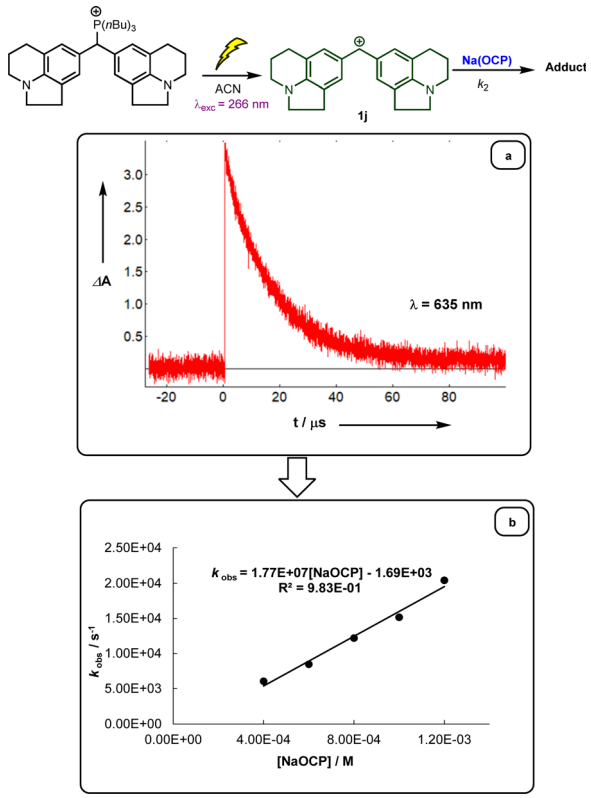

Fig. 1 (a) Decay of the absorbance of carbocation **1j** obtained after irradiation of a 3.07×10^{-5} mol L^{-1} solution of the phosphonium salt **1j-P(*n*Bu)$_3$** in acetonitrile in the presence of Na(OCP). (b) Plot of the pseudo-first-order rate constants k_{obs} (s^{-1}) *versus* the concentration of Na(OCP).

Table 2 Second-order rate constants for the reaction of [OCP$^-$] with reference electrophile in acetonitrile at 20 °C

Electrophile	k_2 (M^{-1} s^{-1})
1a	—[a]
1b	—[a]
1c	2.52×10^9
1d	2.18×10^9
1e	—
1f	1.04×10^8
1g	9.67×10^7
1h	2.23×10^8
1i	1.08×10^8
1j	1.77×10^7
1k	1.74×10^4
1l	2.98×10^2
1m	2.17×10^2
1n	3.71×10^1

[a] Very fast reaction.

counterion does not play a crucial role in the reactivity of [OCP]$^-$ towards carbocations (see ESI‡). The effect of dioxane on the reactivity has also been addressed, and we found that the reaction of dioxane-free Na(OCP) with **1n** react similarly as [Na(OCP)][(dioxane)$_{2.5}$].

In accordance with eqn (1), Fig. 2 shows that the second-order rate constants k_2 correlate linearly with the electrophilicity parameters E of the reference electrophiles **1**. The flattening of the curve at $k_2 \approx 2.5 \times 10^9$ L mol^{-1} s^{-1} is obviously due to diffusion control, which is in agreement with previous observations by Mayr *et al.* for the reactions of other benzhydrylium ions with other nucleophiles.[19b] The nucleophilicity parameters ($N = 19.02$ and $s_N = 0.82$) of [OCP]$^-$ were derived from the linear part of the curve (*i.e.*, reactions with **1h–1n** in Fig. 2).

It should be noted that the measured second-order rate constants (Table 2) could not be attributed to a single electron transfer mechanism, as the oxidation of Na(OCP) is known to yield the heterobicyclic dianion, $(P_4C_4O_4)^{2-}$. This intermediate was not observed by ^{31}P NMR when we investigated the reaction of Na(OCP) with various carbocations **1**.

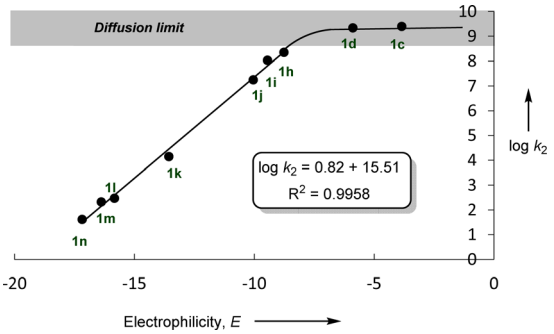

Fig. 2 Plot of log k_2 for the reactions of sodium phosphaethynolate Na(OCP) with reference electrophiles **1**, in acetonitrile at 20 °C *versus* their electrophilicity parameters E.

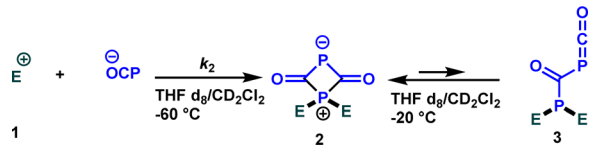

Scheme 3 Reactions of Na(OCP) with carbocations **1b** and **1e**.

It is important to emphasize the excellent linearity observed in the correlation ($\log k_2$ *vs.* E), indicating that the rate-determining step does not change throughout this reaction series. This implies that the same nucleophile terminus center attacks all electrophiles.

The next critical step involves determining whether the identified nucleophilicity parameters align with the attack on oxygen or phosphorus. To elucidate this aspect, we investigated the reaction outcomes of Na(OCP) with both the highly reactive electrophile **1b** as well as the stabilized carbocation **1e** (Scheme 3).

When Na(OCP) (1.2 equivalents) reacted with one equivalent of carbocation **1e** in a dichloromethane/THF (1 : 1) mixture at room temperature, a complex ^{31}P NMR spectrum was obtained. However, when the same reaction was carried out at low temperature (−60 °C), an immediate disappearance of the Na(OCP) ($\delta^{31}P\{^1H\}$ = −394.1 ppm) was observed within five minutes and a new species bearing two phosphorus atoms appeared ($\delta^{31}P\{^1H\}$ = 341.8 ppm (d, $^2J_{PP}$ = 36.7 Hz) and 121.2 ppm (d, $^2J_{PP}$ = 36.7 Hz)). ^{1}H, ^{13}C and 2D NMR experiments indicated the exclusive formation of the zwitterion **2**. The same intermediate was also detected for other electrophiles **1** (for more information, see ESI‡). When the temperature was raised to −20 °C, the zwitterion **2** coexists with the phosphaketene adduct **3** ($\delta^{31}P\{^1H\}$ = −276.2 ppm (d, $^2J_{PP}$ = 167.7 Hz) and 21.1 ppm (d, $^2J_{PP}$ = 167.8 Hz)) in 5 to 1 ratio (**2**/**3**).

Grützmacher, Stephan, and co-authors reported the formation of structurally analogous complexes when they studied the reactions of the phosphaethynolate anion with a variety of boranes as Lewis acids.[20]

To understand how these intermediates **2** and **3** were formed and to support the analysis of the kinetic data, we analyzed putative reaction mechanisms for the combination of free $[OCP]^-$ with the tropylium cation **1b** using density functional theory (RI-DSD-PBEP86-D3(BJ)/def2-QZVPP/SMD(THF)//M06-2X/6-31+G(d,p)/SMD(THF)). These results are summarized together with selected transition state structures in Scheme 4. Our calculations predict that $[OCP]^-$ and **1b** initially form a reactant complex [**OCP**/**1b**] that is more stable than the separated reactants. This complex is most likely held together *via* coulombic interactions. However, due to the large number of potential conformers of the reactant complex, the energetic value for this complex in Scheme 4 corresponds to the optimized structure at the end of the corresponding IRC calculation. Therefore, it is not unlikely that there are more stable bimolecular complexes. Within this complex, the OCP anion undergoes a rapid reaction with the tropylium ion (**TS1**, $\Delta G^‡$ = 10 kJ mol^{-1}) and forms the P-alkylated intermediate **4b**. This is in perfect agreement with the high nucleophilicity (see above) and electrophilicity (E = −3.72)[17] of the tropylium ion. The alternate reactivity at the oxygen atom of $[OCP]^-$ (not shown in Scheme 4) leads to an *O*-alkylated compound that lies 101 kJ mol^{-1} above intermediate **5b**.

In the next steps, **4b** is transformed into the experimentally observed intermediate **2b**. This requires the reaction with another $[OCP]^-$ and a second tropylium cation. According to our DFT calculations, the formal [2 + 2] cycloaddition between $[OCP]^-$ and **4b** proceeds in a stepwise fashion and occurs very quickly (**TS2**, **TS3**, $\Delta G^‡$ = 21 and 34 kJ mol^{-1}) and forms the diphosphetanedione **6b**. In this sequence, another $[OCP]^-$ will initially attack the electrophilic carbon atom within phosphaketene **4b**. This is followed by a ring-closing reaction to yield the diphosphetanedione anion **7b**. Alkylation of **7b** with a second equivalent of the tropylium cation again proceeds very rapidly and can occur at both phosphorus atoms through **TS4** or **TS5**. While negative barriers were calculated on the RI-DSD-PBEP86 potential energy surface in both cases, small barriers were determined on the M06-2X surface. Eventually, the zwitterion **2b** is formed with a high thermodynamic driving force (ΔG = −196 kJ mol^{-1}) as the more stable species.

Alternatively, intermediate **4b** can first react with the tropylium ion through **TS6**, which requires a slightly larger barrier of 64 kJ mol^{-1}. No transition states could be located on the potential energy surface for the reaction of **5b** with the OCP anion and all potential energy surface scans resulted in a barrierless addition. This indicates that this step will proceed very rapidly under the reaction conditions. Cyclization of phosphaketene **3b** finally results in the zwitterion **2b** again without a significant barrier. In agreement with the experimental observations (Scheme 3), the computational investigations also indicate that zwitterion **2b** is more stable than the phosphaketene **3b**, however, the thermodynamic difference seems to be substantially overestimated in the calculations. To better understand this deviation, we first calculated the thermodynamic differences for other substituents on the phosphorus atom (see the ESI for details‡). Regardless of the substituent, a comparable strong preference for the zwitterions was observed in all cases. Similarly, different computational methods (*e.g.*, DLPNO-CCSD(T), B2GP-PLYP, M06-2X, ω97X-V) also resulted in almost identical energy differences in favor of the zwitterion. Finally, we realized that solvation seems to be an important aspect. In the gas phase, both structures **2b** and **3b** are almost isoenergetic, and with increasing polarity, the zwitterion **2b** substantially benefits from solvation, which then leads to an overestimation. Thus, the overestimation can be traced back to issues arising from the charge separation within the zwitterions.

These results seem to contradict earlier observations by Slootweg and coworkers, who reported a different product for the reaction of sodium phosphaethynolate with 1,2,3-tris-*tert*-butylcyclopropenium tetrafluoroborate **1o** (Scheme 5).[11j] Indeed, while the first step of the reaction leads to a phosphaketene, similar to the reaction with our reference electrophiles **1**, a fast [2 + 2] cycloaddition yields bis(cyclo-propenyl) diphosphetanedione **8o**. The different reactivity of these

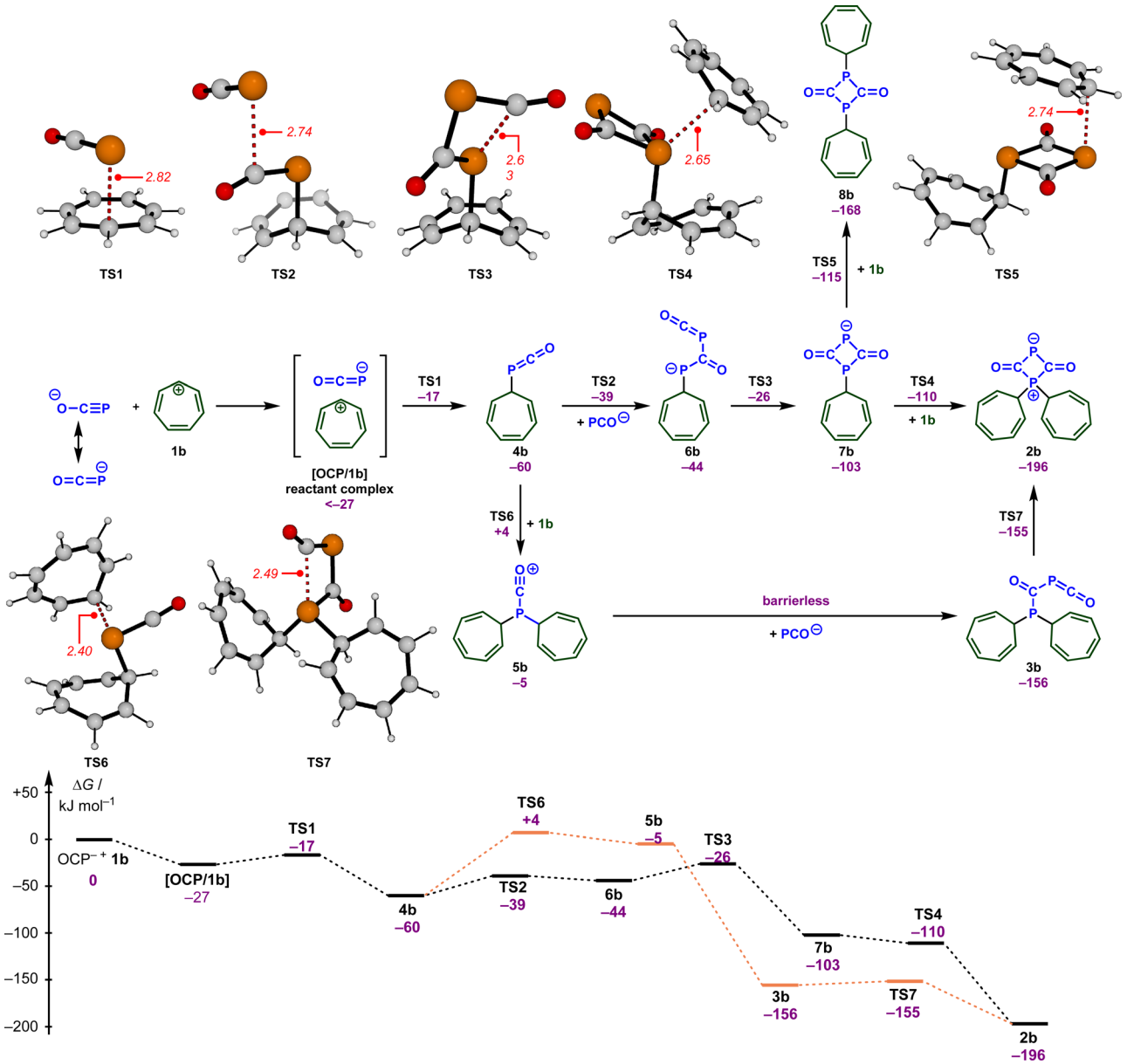

Scheme 4 Calculated reaction free energies (in kJ mol^{-1}) and selected transition states (bond lengths in Å) for the proposed reaction mechanism for the formation of the zwitterion **2b** and the phosphaketene **3b**.

electrophiles is probably caused by the steric demand within **1o**. While the 1,3-disubstituted diphosphetandione **8b** is thermodynamically less stable than the zwitterion **2b** (see Scheme 4), the situation reverts for the electrophile **1o**. According to our calculations, **8o** is substantially more stable than **2o** ($\Delta\Delta G$ = −48 kJ mol^{-1}) (Scheme 5).

Based on the results highlighted above, one can assign the measured nucleophilicity (N = 19.02, s_N = 0.82) to the phosphorus site of the phosphaethynolate, which is five orders of magnitude more reactive than cyanate anion[21] and ten times more reactive than the N-terminus of thioisocyanate.[22] This high reactivity may explain the capability of this anion to react with a wide variety of electrophiles, including weak ones such as carbodiimide ($E \approx -20$) (Fig. 3).[23,24]

After determining the phosphorus nucleophilicity of the OCP anion, we now wondered how this knowledge can be used in synthetically useful transformations. The investigation of the mechanism of the reaction of sodium phosphaethynolate with stabilized carbocations, for instance **1b**, revealed the formation of the zwitterion **2b** that was detected at −60 °C. To convert the latter into an isolable intermediate, we treated it with the NHC carbene **9**. Notably, this resulted in the formation of azolium phosphaenolate **10b** in quantitative yield, which can be described as the NHC adduct of **4b**. The structure of **10b** was confirmed by a single crystal X-ray diffraction experiment (Scheme 6). In the solid state, the C–P and C–O bond lengths are 1.737 and 1.264 Å, respectively. These results are in good agreement with those reported by Stephan, Cummins *et al.*[25] for

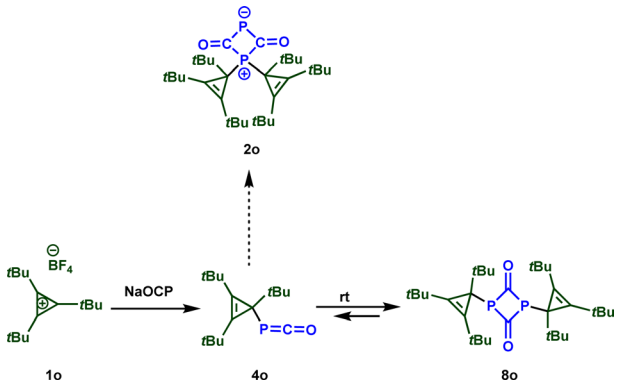

Scheme 5 Reaction of sodium phosphaethynolate with 1,2,3-tris-*tert*-butylcyclopropenium **1o**.[11j]

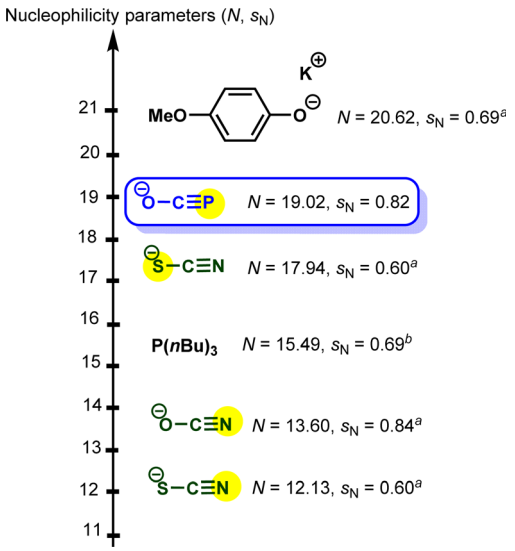

Fig. 3 Embedding sodium phosphaethynolate in the Mayr nucleophilicity scale. [a] Solvent: acetonitrile. [b] Solvent: dichloromethane.[21–24]

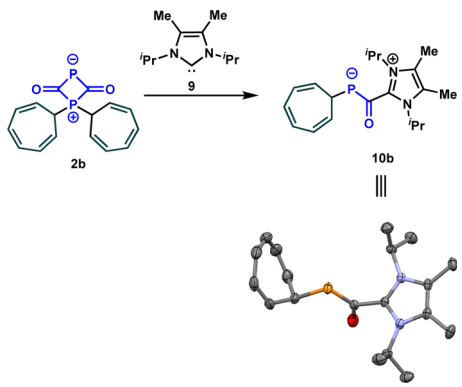

Scheme 6 Reaction of the zwitterion **2b** with the carbene **9**.

acylphosphide anions, where experimental and computational studies revealed that the short C–P and long C–O bond are the consequence of the delocalization of electron density from the phosphide lone pair into π*(C═O) orbital.

Importantly, when the zwitterion **2e** is dissolved in (dichloromethane/THF) in the presence of 0.5 equiv. of water, the secondary phosphine **11e** is formed, as observed by ^{31}P NMR spectroscopy (see ESI‡). Conducting the reaction in the presence of D_2O resulted in the formation of deuterated phosphine, providing confirmation that the proton originates from water (Scheme 7).

Building upon these observations, we combined different stabilized carbocations **1** with Na(OCP) in THF/dichloromethane (1 : 1) mixture, containing 0.5 equiv. of water. Notably, employing stabilized carbocations (**1c, f, g, i, j**) led to the formation of secondary phosphines **11** and secondary phosphine oxides **12** in good to excellent yields, as confirmed by ^{31}P NMR. While the phosphine **11e** is stable to be isolated by column chromatography, the other phosphines oxidize rapidly when exposed to air. Consequently, these were treated with 5 equivalents of H_2O_2 and isolated as secondary phosphine oxides **12** in synthetically useful yields (Scheme 7).

Due to the high electrophilicity and Lewis acidity of **1a** and **1b**,[19a] their reactions with the OCP anion produced a mixture of secondary and tertiary phosphines. Clearly, the formed secondary phosphines promptly react with **1a** and **1b** to give the tertiary phosphines. Both phosphines are oxidized to the phosphine oxides and isolated separately. The overall isolated yields are consistently good to very good (Scheme 8).

It is important to note that while an elegant synthesis of acyl phosphines and related molecules from the phosphaethynolate anion and related structures from $[OCP]^-$ has been previously documented by Goicoechea,[11b] Stephan,[26] and others, direct synthesis of the sterically hindered phosphines **12** at **13** has not been described to our knowledge. Furthermore, traditional methods for obtaining these types of molecules would necessitate the use of strong Brønsted bases. Therefore, this approach offers a more convenient route as it enables access to these compounds under mild and sustainable conditions.

We again relied on DFT calculations to gain further insights into the mechanism of this useful transformation (Scheme 9). To simplify the computational studies, we continue to use the tropylium cation **1b** as the initial electrophile. Based on our DFT calculations, the formation of the secondary phosphine **11b**, CO_2, and phosphaneylidenemethanone (OCPH) is thermodynamically feasible ($\Delta G = -40$ kJ mol^{-1}). Mechanistically, we propose that the zwitterion **2b** initially reacts with water to yield intermediate **14**. No barrier could be detected for the attack of water and the computational studies indicate that the attack of water and the proton transfer from water to the phosphorus atom occurs in a concerted fashion. This intermediate quickly looses OCPH *via* **TS8** and affords the phosphanecarboxylic acid **15**. A concerted decarboxylation is generally feasible and affords the secondary phosphine **11b** in an overall favorable process, but the barrier for this step is very high (**TS9**, $\Delta G^{\ddagger} = 155$ kJ mol^{-1}). Thus, a concerted process is very unlikely under the reaction conditions. Instead, the OCP anion could deprotonate the carboxylic acid and the decarboxylation takes place through an anionic transition state **TS10** ($\Delta G^{\ddagger} = 125$ kJ mol^{-1}). This is still a substantial barrier, but might be slightly overestimated due to the involved proton transfer. A more likely

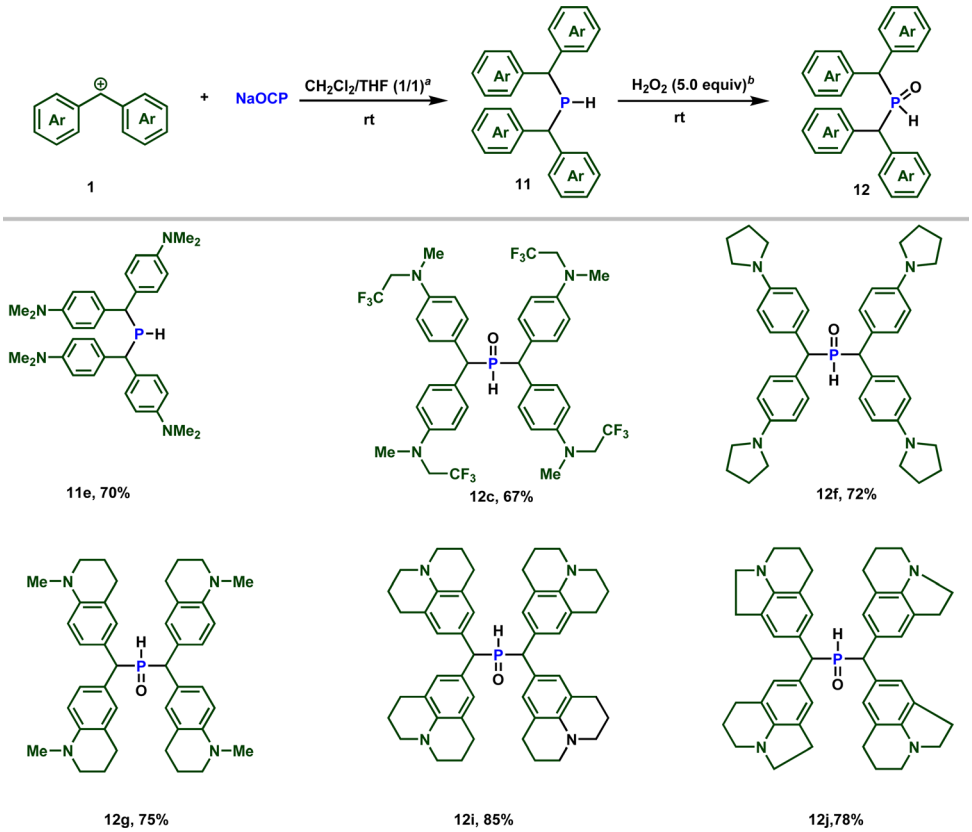

Scheme 7 Reactivity of sodium phosphaethynolate towards stabilized carbocations. [a] 0.5 equiv. of water. [b] H_2O_2 30% (w/w) in water was used.

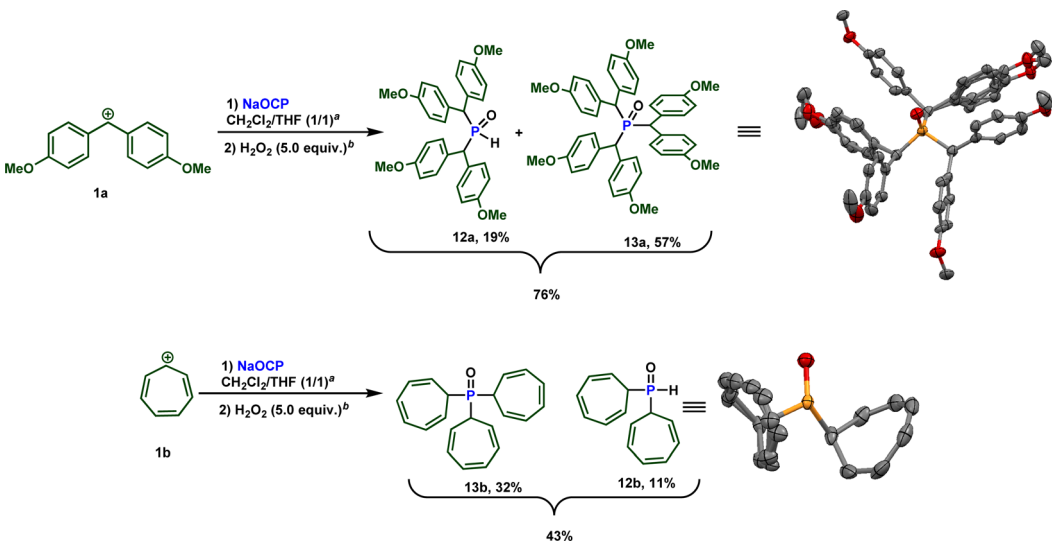

Scheme 8 Reactivity of sodium phosphaethynolate towards highly reactive carbocations **1a** and **1b**. [a] 0.5 equiv. of water. [b] H_2O_2 30% (w/w) in water was used.

scenario is the formation of a zwitterionic phosphanecarboxylic acid **16**. Although a formal 1,3 proton shift through **TS11** is very unfavorable, another molecule **15** or the OCP anion will facilitate the proton transfer. The zwitterion **16** readily undergoes the decarboxylation (**TS12**) and affords the secondary phosphane in a very rapid reaction.

We should emphasize that consistent with the computational studies, the formation of OCPH was experimentally confirmed, as its dimer was detected when **2b** was reacted with water (0.5 equiv.) at −60 °C (see ESI,‡ pages S93 and S94) (^{31}P $\{^1$H$\}$ NMR spectrum at 305.8 and 75.9 ppm with a $^2J_{P-P}$ coupling constant of 16.0 Hz, as well as a doublet of doublets at 7.32 ppm

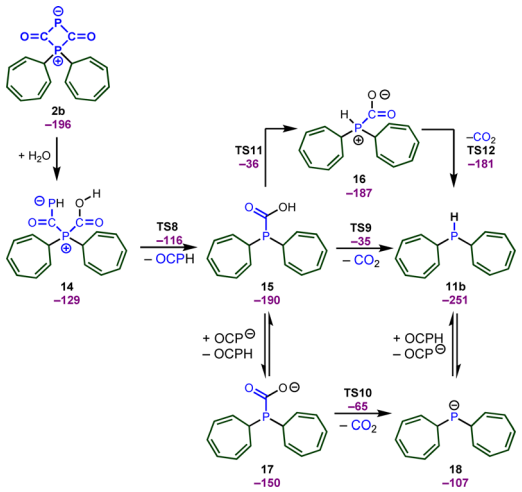

Scheme 9 Potential pathways for the formation of secondary phosphines.

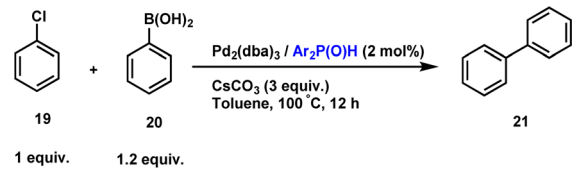

$Ar_2P(O)H$:	12a	12b	12c	12i	$Ph_2P(O)H$
NMR yield:	68%	55%	77%	72%	-

Scheme 10 Secondary phosphine oxide/$Pd_2(dba)_3$ catalysed the Suzuki cross-coupling reaction of **19** with **20**.

($^1J_{P-H}$ = 172, $^3J_{P-H}$ = 16.0 Hz)). This finding aligns well with Goicoechea's observation that OCPH undergoes dimerization.[27]

Finally, given that hindered secondary phosphine oxides have proven to be effective ligands for transition metal-catalyzed reactions, as initially demonstrated by Li,[28] we evaluated their combination with $Pd_2(dba)_3$ in the Suzuki cross-coupling reaction of aryl chloride **19** with phenylboronic acid **20**.[29] Importantly, the desired biphenyl product **21** in good yields, showing the efficiency of our secondary phosphine oxides (Scheme 10). Interestingly, no reaction occurred when diphenylphosphine oxide was used as a ligand, highlighting the crucial role of sterically hindered phosphines.

Conclusions

In conclusion, we herein provide an experimental quantification of the phosphorus nucleophilicity of the sodium phosphaethynolate. This reactivity is both kinetically and thermodynamically favourable. Mechanistic investigations allowed the identification and full characterization of key intermediates such as the zwitterion **2**, and also the optimization of experimental conditions enabling the synthesis of synthetically useful organophosphorus molecules such as sterically hindered secondary phosphines oxides. The latter have shown to be effective ligands in Suzuki cross coupling reaction.

Data availability

All experimental procedures, details of the calculations, and additional data can be found in the ESI.‡

Author contributions

T. H. V. N. conducted synthetic and kinetic experiments, while S. C. analysed the kinetic data and carried out experiments using laser-flash photolysis equipment. S. M.-L. conducted the X-ray experiments. M. B. performed all calculations. S. L. conceived and supervised the project. All authors participated in discussing the results, providing comments, and proof-reading the manuscript.

Conflicts of interest

The authors declare no competing interests.

Acknowledgements

The authors are grateful to the generous support from the "Ministère de la Recherche et des Nouvelles Technologies" (allocation to T. H. V. N.), the CNRS, the Agence Nationale de la Recherche (ANR, PhotoFlat No. 220424), the University of Toulouse III Paul Sabatier, and Deutsche Forschungsgemeinschaft (DFG, German Research Foundation, BR5154/4-1), for financial support. The authors express their gratitude to Dr Nicolas Mézailles (LHFA-Toulouse) and Dr David Leboeuf (ISIS-Strasbourg) for his valuable discussions and suggestions.

Notes and references

1 D. E. C. Corbridge, *Phosphorus 2000. Chemistry, Biochemistry & Technology*, Elsevier, Amsterdam, 2002.
2 (*a*) W. Schipper, *Eur. J. Inorg. Chem.*, 2014, 1567–1571; (*b*) F. H. Westheimer, *Science*, 1987, **235**, 1173–1178; (*c*) D. M. Karl, *Nature*, 2000, **406**, 31–33; (*d*) L. V. Kochian, *Nature*, 2012, **488**, 466–467.
3 K. H. Büchel, H. H. Moretto and P. Woditsch, *Industrial Inorganic Chemistry*, Wiley VCH, New York, 2nd edn, 2000, pp. 65–101.
4 For a comprehensive review on phosphinate chemistry, see: J. L. Montchamp, *Acc. Chem. Res.*, 2014, **47**, 77–87.
5 (*a*) D. J. Scott, *Angew. Chem., Int. Ed.*, 2022, **61**, e202205019; (*b*) D. J. Scott, J. Cammarata, M. Schimpf and R. Wolf, *Nat. Chem.*, 2021, **13**, 458–464; (*c*) M. Till, J. Cammarata, R. Wolf and D. J. Scott, *Chem. Commun.*, 2022, **58**, 8986–8989; (*d*) J. E. Borger, A. W. Ehlers, J. C. Slootweg and K. Lammertsma, *Chem.–Eur. J.*, 2017, **23**, 11738–11746; (*e*) M. Scheer, G. Balázs and A. Seitz, *Chem. Rev.*, 2010, **110**, 4236–4256; (*f*) B. M. Cossairt, N. A. Piro and C. C. Cummins, *Chem. Rev.*, 2010, **110**, 4164–4177.

6 (*a*) J. M. Goicoechea and H. Grützmacher, *Angew. Chem., Int. Ed.*, 2018, **57**, 16968–16994; (*b*) Z. J. Quan and X. C. Wang, *Org. Chem. Front.*, 2014, **1**, 1128–1131; (*c*) Z. Quan, W. Wang and X. Wang, *Chin. J. Org. Chem.*, 2015, **35**, 2301–2312.

7 (*a*) M. Regitz, *Chem. Rev.*, 1990, **90**, 191–213; (*b*) K. B. Dillon, F. Mathey and J. F. Nixon, *Phosphorus: The Carbon Copy*, Wiley, Chichester, 1998.

8 For phosphaketenes obtained from OCP anion, see: (*a*) S. Alidori, D. Heift, G. Santiso-Quinones, Z. Benkő, H. Grützmacher, M. Caporali, L. Gonsalvi, A. Rossin and M. Peruzzini, *Chem.–Eur. J.*, 2012, **18**, 14805–14811; (*b*) L. Liu, D. A. Ruiz, F. Dahcheh, G. Bertrand, R. Suter, A. M. Tondreau and H. Grützmacher, *Chem. Sci.*, 2016, **7**, 2335–2341; (*c*) N. Del Rio, A. Baceiredo, N. Saffon-Merceron, D. Hashizume, D. Lutters, T. Müller and T. Kato, *Angew. Chem., Int. Ed.*, 2016, **55**, 4753–4758; (*d*) Y. Xiong, S. Yao, T. Szilvási, E. Ballestero-Martínez, H. Grützmacher and M. Driess, *Angew. Chem., Int. Ed.*, 2017, **56**, 4333–4336.

9 (*a*) G. Becker, W. Schwarz, N. Seidler and M. Westerhausen, *Z. Anorg. Allg. Chem.*, 1992, **612**, 72–82; (*b*) G. Becker, G. Heckmann, K. Hübler and W. Schwarz, *Z. Anorg. Allg. Chem.*, 1995, **621**, 34–46.

10 (*a*) F. F. Puschmann, D. Stein, D. Heift, C. Hendriksen, Z. A. Gal, H. F. Grützmacher and H. Grützmacher, *Angew. Chem., Int. Ed.*, 2011, **50**, 8420–8423; (*b*) D. Heift, Z. Benkő and H. Grützmacher, *Dalton Trans.*, 2014, **43**, 831–840; (*c*) I. Krummenacher and C. C. Cummins, *Polyhedron*, 2012, **32**, 10–13; (*d*) A. R. Jupp and J. M. Goicoechea, *Angew. Chem., Int. Ed.*, 2013, **52**, 10064–10067.

11 For selected examples on the use of OCP anion in organic and organometallic chemistry, see: (*a*) A. M. Tondreau, Z. Benkő, J. R. Harmer and H. Grützmacher, *Chem. Sci.*, 2014, **5**, 1545–1554; (*b*) A. R. Jupp and J. M. Goicoechea, *J. Am. Chem. Soc.*, 2013, **135**, 19131–19134; (*c*) Y. H. Wu, Z. F. Li, W. P. Wang, X. C. Wang and Z. J. Quan, *Eur. J. Org Chem.*, 2017, 5546–5553; (*d*) R. Suter, Y. Mei, M. Baker, Z. Benkő, Z. Li and H. Grützmacher, *Angew. Chem., Int. Ed.*, 2017, **56**, 1356–1360; (*e*) C. Camp, N. Settineri, J. Lefèvre, A. R. Jupp, J. M. Goicoechea, L. Maron and J. Arnold, *Chem. Sci.*, 2015, **6**, 6379–6384; (*f*) C. J. Hoerger, F. W. Heinemann, E. Louyriac, L. Maron, H. Grützmacher and K. Meyer, *Organometallics*, 2017, **36**, 4351–4354; (*g*) L. Liu, D. A. Ruiz, D. Munz and G. Bertrand, *Chem*, 2016, **1**, 147–153; (*h*) D. W. N. Wilson, A. Hinz and J. M. Goicoechea, *Angew. Chem., Int. Ed.*, 2018, **57**, 2188–2193; (*i*) L. Liu, D. A. Ruiz, F. Dahcheh, G. Bertrand, R. Suter, A. M. Tondreauc and H. Grützmacher, *Chem. Sci.*, 2016, **7**, 2335–2341; (*j*) T. Krachko, A. W. Ehlers, M. Nieger, M. Lutz and J. C. Slootweg, *Angew. Chem., Int. Ed.*, 2018, **57**, 1683–1687; (*k*) M. G. Jafari, Y. Park, B. Pudasaini, T. Kurogi, P. J. Carroll, D. M. Kaphan, J. Kropf, M. Delferro, M. Baik and D. J. Mindiola, *Angew. Chem., Int. Ed.*, 2021, **60**, 24411–24417; (*l*) M. M. Hansmann, *Chem.–Eur. J.*, 2018, **24**, 11573–11577.

12 D. Heift, Z. Benkő and H. Grützmacher, *Dalton Trans.*, 2014, **43**, 5920–5928.

13 Á. Horváth, B. D. Lőrincz and Z. Benkő, *Chem. Eur. J.*, 2023, **29**, e2023006.

14 H. Mayr, M. Breugst and A. R. Ofial, *Angew. Chem., Int. Ed.*, 2011, **50**, 6470–6505.

15 (*a*) R. G. Pearson, *Science*, 1966, **151**, 172–177; (*b*) R. G. Pearson, *J. Am. Chem. Soc.*, 1963, **85**, 3533–3539; (*c*) R. G. Pearson and J. Songstad, *J. Am. Chem. Soc.*, 1967, **89**, 1827–1936.

16 H. Mayr and A. R. Ofial, *SAR QSAR Environ. Res.*, 2015, **26**, 619–646.

17 H. Mayr, K.-H. Müller, A. R. Ofial and M. Bühl, *J. Am. Chem. Soc.*, 1999, **121**, 2418–2424.

18 (*a*) H. Mayr and M. Patz, *Angew. Chem., Int. Ed.*, 1994, **33**, 938–957; (*b*) H. Mayr, T. Bug, M. F. Gotta, N. Hering, B. Irrgang, B. Janker, B. Kempf, R. Loos, A. R. Ofial, G. Remennikov and H. Schimmel, *J. Am. Chem. Soc.*, 2001, **123**, 9500–9512; (*c*) H. Mayr, B. Kempf and A. R. Ofial, *Acc. Chem. Res.*, 2003, **36**, 66–77; (*d*) *The database of Mayr reactivity parameters (N, s_N, and E)*, **https://www.cup.lmu.de/oc/mayr/reaktionsdatenbank2/**, accessed 27/05/2024.

19 (*a*) H. Mayr, J. Ammer, M. Baidya, B. Maji, T. A. Nigst, A. R. Ofial and T. Singer, *J. Am. Chem. Soc.*, 2015, **137**, 2580–2599; (*b*) J. Ammer, C. Nolte and H. Mayr, *J. Am. Chem. Soc.*, 2012, **134**, 13902–13911; (*c*) J. Ammer, C. F. Sailer, E. Riedle and H. Mayr, *J. Am. Chem. Soc.*, 2012, **134**, 11481–11494; (*d*) R. Loos, S. Kobayashi and H. Mayr, *J. Am. Chem. Soc.*, 2003, **125**, 14126–14132; (*e*) J. Ammer and H. Mayr, *J. Phys. Org. Chem.*, 2013, **26**, 956–969.

20 K. M. Szkop, A. R. Jupp, R. Suter, H. Grützmacher and D. W. Stephan, *Angew. Chem., Int. Ed.*, 2017, **56**, 14174–14177.

21 A. A. Tishkov and H. Mayr, *Angew. Chem., Int. Ed.*, 2005, **44**, 142–145.

22 R. Loos, S. Kobayashi and H. Mayr, *J. Am. Chem. Soc.*, 2003, **125**, 14126–14132.

23 L. Liu, J. Zhu and Y. Zhao, *Chem. Commun.*, 2014, **50**, 11347–11349.

24 For the electrophilicity of carbodiimides, see: Z. Li, R. J. Mayer, A. R. Ofial and H. Mayr, *J. Am. Chem. Soc.*, 2020, **142**, 8383–8402.

25 K. M. Szkop, M. B. Geeson, D. W. Stephan and C. C. Cummins, *Chem. Sci.*, 2019, **10**, 3627–3631.

26 (*a*) K. M. Szkop, A. R. Jupp, H. Razumkov and D. W. Stephan, *Dalton Trans.*, 2020, **49**, 885–890; (*b*) D. A. Petrone, K. M. Szkop, L. Miao, P. S. Onge, Z. W. Qu, S. Grimme and D. W. Stephan, *Angew. Chem., Int. Ed.*, 2021, **60**, 18547–18551.

27 A. Hinz, R. Labbow, C. Rennick, A. Schulz and J. M. Goicoechea, *Angew. Chem., Int. Ed.*, 2017, **56**, 3911–3915.

28 G. Y. Li, *J. Org. Chem.*, 2002, **67**, 3643–3650.

29 (*a*) T. M. Shaikh, Ch-M. Weng and F.-E. Hong, *Coord. Chem. Rev.*, 2012, **256**, 771–803; (*b*) A. Gallen, A. Riera, X. Verdaguer and A. Grabulosa, *Catal. Sci. Technol.*, 2019, **9**, 5504–5561.